

Formic Acid Dehydrogenation

Iodide-Promoted Dehydrogenation of Formic Acid on a Rhodium Complex

Zhijun Wang,^[a,b,c] Sheng-Mei Lu,^[b] Jianjun Wu,^[a] Can Li,^{*[b]} and Jianliang Xiao^{*[a]}

Abstract: Efficient and simple catalyst systems for dehydrogenation of formic acid (FA) to produce hydrogen are always desirable. In this work, the catalytic dehydrogenation of FA to H₂ and CO₂ by using the readily available [RhCp*Cl₂]₂ was found to be accelerated simply by the addition of halide anions, iodide being the most effective. At 60 °C, with [RhCp*Cl₂]₂ in

azeotropic FA and triethylamine (TEA), the initial turnover frequency of dehydrogenation in the presence of I⁻ (4375 h⁻¹) is seven times as high as that of the reaction without additive (625 h⁻¹). Preliminary mechanistic studies suggest that the dehydrogenation is turnover-limited by the hydride-formation step, which could be facilitated by the presence of I⁻.

Introduction

Hydrogen generation from formic acid (FA) has attracted much attention in recent years.^[1] This reaction could provide a technology for supplying hydrogen to, for example, small mobile or stationary applications. Accordingly, studies on the catalytic dehydrogenation of FA have been carried out by a number of research groups, some reporting excellent turnover frequencies (TOFs).^[2–4] In the area of homogeneous catalysis, the highest TOF of 487,500 h⁻¹ was demonstrated by Li et al.,^[4i] who used a [Cp*Ir(L)Cl]Cl catalyst (Cp* = pentamethylcyclopentadienide; L = 2,2'-bi-2-imidazoline). As with this catalyst developed by Li et al., most of the reported catalysts comprise relatively complicated or expensive bidentate/tridentate ligands attached to the metal center. Although they can be highly active in the dehydrogenation reaction, considering the practicality of the reaction in real life, developing efficient catalyst systems without complicated or delicate ligands would be preferable.

Halide ions, one of the most common and simple additives and ancillary ligands for transition metal complexes used in catalysis, have frequently been found to exert some unusual influence on catalytic reactions.^[5] In particular, the significant promoting effect of the iodide anion in hydrogenation and transfer-hydrogenation reactions has been recognized.^[5b,6] Although

the mechanistic details of the effect of the iodide ion on these reactions remain unclear, its softness, *trans*-effect, and size may play a role. Here we have observed that halide anions can accelerate the FA dehydrogenation catalyzed by [RhCp*Cl₂]₂ in the FA–triethylamine (TEA) azeotrope. The most effective halide ion is I⁻, and it enhances the reaction rate by seven times with an increase in the initial TOF from 625 to 4375 h⁻¹ at 60 °C. A preliminary mechanistic study suggests that the dehydrogenation is turnover-limited by hydride formation and the iodide anion facilitates this step while prolonging the catalyst lifetime.

Results and Discussion

Formic Acid Dehydrogenation

The precatalyst [RhCp*Cl₂]₂ has been shown to catalyze the transfer hydrogenation of N-heterocycles with the FA–TEA (FT) azeotrope in the presence of halide ions and particularly iodide.^[6] Hydrogen results from the decomposition of FA; thus the combination of [RhCp*Cl₂]₂ and X⁻ is capable of FA dehydrogenation. At the starting point, we therefore examined the dehydrogenation of FA catalyzed by [RhCp*Cl₂]₂ in the absence or presence of halide anions at 60 °C in the FT azeotrope, where the FA/TEA mol ratio is 2.5. The amount of evolved gas was determined by the water displacement method, and gas chromatography confirmed the products to be H₂ and CO₂ (in a 1:1 ratio) with a negligible level of CO (Figure S1). As shown in Table 1 and Figure 1, both the TOF and TON are increased upon the addition of potassium halides, KI enabling the fastest reaction. In the presence of KI, the initial TOF increased most significantly to 4375 h⁻¹ from 625 h⁻¹ without any halide additive. Comparing the TOF values obtained with KI, NaI, and LiI, we concluded that this enhancement arises from the halide anions rather than the alkali cations. In addition, the presence of I⁻ makes this catalyst more productive, increasing the TON from 151 to 706 (at 40 % FA conversion, Table 1, entries 1 and 5) after 30 min.

[a] Liverpool Centre for Materials & Catalysis,
Department of Chemistry, University of Liverpool,
Liverpool L69 7ZD, UK
E-mail: J.Xiao@liverpool.ac.uk
<http://pcwww.liv.ac.uk/~jxiao/>

[b] State Key Laboratory of Catalysis,
Dalian Institute of Chemical Physics,
Chinese Academy of Sciences,
457 Zhongshan Road, Dalian 116023, China
E-mail: canli@dicp.ac.cn
<http://www.canli.dicp.ac.cn/>

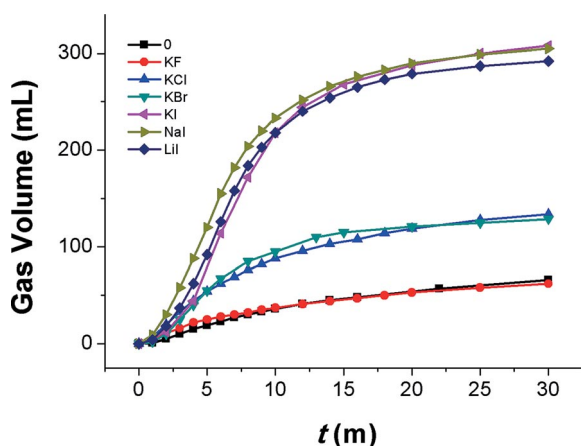
[c] Graduate University of Chinese Academy of Sciences,
Beijing 100049, China

Supporting information for this article is available on the WWW under
<http://dx.doi.org/10.1002/ejic.201501061>.

Table 1. Dehydrogenation of FA in the presence of different alkali halide salts.^[a]

Entry	Additive	Gas [mL] ^[b]	TON (30 min) ^[b]	Conversion	TOF _{max} [h ⁻¹] ^[c]
1	–	66	151	9 %	625
2	KF	62	142	8 %	875
3	KCl	134	307	17 %	1625
4	KBr	129	296	17 %	2009
5	KI	308	706	40 %	4375
6	NaI	305	699	40 %	4375
7	LiI	292	669	38 %	4250

[a] General reaction conditions: 5.0 μmol of $[\text{RhCp}^*\text{Cl}_2]_2$, 1.0 mmol of alkali halide, 1.5 mL of FT azeotrope, 60 °C. Approximately 16 mmol of FA is present in 1.5 mL of FT azeotrope. [b] The amount of gas was recorded and the TON was calculated after 30 min reaction. [c] TOF_{max} was calculated on the basis of the volume of evolved gas from 3 to 6 min after the beginning of the reaction, to rule out the influence of temperature fluctuation due to the injection of FT solution and to avoid the initial induction period (Figure 1). Each reaction was repeated at least twice with an error less than 5 %. No reaction was observed without catalyst.

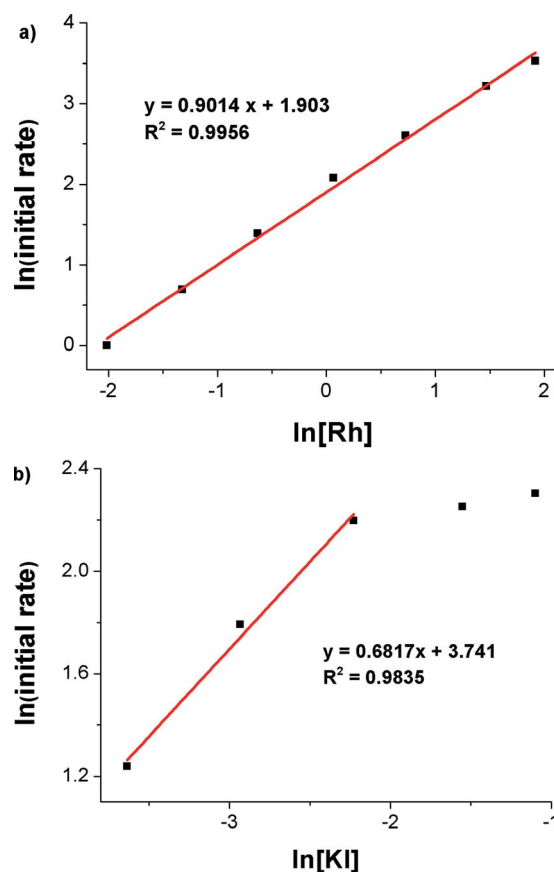
Figure 1. Time course of gas evolution during the dehydrogenation of FA in the presence of various inorganic salts (5.0 μmol of $[\text{RhCp}^*\text{Cl}_2]_2$, 1.0 mmol of inorganic salts (6 mol-%), 1.5 mL of FT azeotrope, 60 °C).

Other rhodium complexes, as well as those based on iridium and ruthenium, were also investigated as catalyst precursors in combination with I^- for FA dehydrogenation (see Table S1). All the complexes tested showed very low activity, except for $[\text{Ru}(p\text{-cymene})\text{Cl}_2]_2$, which gave a moderate TOF of 1500 h^{-1} . This value is six times that observed for the reaction without I^- (Table S1, entries 2–3), which indicates that the promoting effect of I^- is not limited to $[\text{RhCp}^*\text{Cl}_2]_2$.

Kinetics of Formic Acid Dehydrogenation

To gain an understanding of the dehydrogenation reaction, the dependence of the rate on temperature, catalyst concentration, amount of KI, and FA/TEA ratio were investigated. The reaction rate increases with temperature, and the temperature dependence of the initial rates follows the Arrhenius equation (Figure S2). The apparent activation energy (E_a) for FA dehydrogenation is estimated to be about 64 kJ mol^{-1} , which is near the typical range of noble-metal-catalyzed hydrogen generation from FA in aqueous solution.^[4g,4h,4i]

The dependence of the rate on catalyst concentration was explored by using 0.1–5.0 μmol of $[\text{RhCp}^*\text{Cl}_2]_2$ in combination with 500 μmol of KI in 1.5 mL of FT azeotrope at 60 °C (Figure S3). The double logarithmic plot of the initial rate against the catalyst concentration shows a linear dependence on $[\text{Rh}]$ (Figure 2a). As shown, the reaction proceeds with an order of 0.90 with respect to the catalyst concentration, $[\text{Rh}]$, which is close to 1.0. This is consistent with the involvement of a mononuclear rhodium species in the catalytic cycle (also see below), and no other polymeric compounds are likely to be the active catalyst. Beyond the $[\text{Rh}]$ concentration of 1.07 mM, the initial TOF declines gradually (Figure S3). This may result from catalyst aggregation at a higher concentration (vide infra).

Figure 2. (a) Plot of $\ln(\text{initial rate of H}_2 \text{ evolution})$ vs. $\ln[\text{Rh}]$ ($[\text{Rh}]$ is the concentration of rhodium monomer). Conditions: 0.1–5.0 μmol of $[\text{RhCp}^*\text{Cl}_2]_2$, 500 μmol of KI, 1.5 mL of FT azeotrope, 60 °C; (b) Plot of $\ln(\text{initial rate of H}_2 \text{ evolution})$ vs. $\ln[\text{KI}]$ (0.8 μmol of $[\text{RhCp}^*\text{Cl}_2]_2$, 40–500 μmol of KI, 1.5 mL of FT azeotrope, 60 °C).

The dependence of the rate on the concentration of KI was investigated by using 0.8 μmol of $[\text{RhCp}^*\text{Cl}_2]_2$ with 40–500 μmol of KI in 1.5 mL of FT azeotrope (Figure S4). The reaction rate shows a fractional order of 0.68 with respect to iodide concentration, up to $[\text{KI}] \approx 0.1 \text{ M}$ ($n_{\text{KI}} = 160 \mu\text{mol}$) (Figure 2b). This result indicates that the iodide ion is likely to be involved in the rate-determining step (RDS) and in the equilibria prior to it.

With different FA/TEA ratios, the time course of gas evolution was recorded as shown in Figure S5. The FT mixtures were prepared with molar ratios of FA/TEA in the range 2.25:1 to 3:1. Figure 3 shows the variation of the initial TOF and TON with

the mol fraction of FA in the starting solution. The final TONs increase approximately linearly with the increase in the amount of FA (blue line). In contrast, the initial TOFs show a reverse dependence on the mol fraction of FA: more FA gives rise to lower TOFs. Since $[\text{HCOO}^-]$ is reversely proportional to $[\text{HCOOH}]$ in the FA/TEA mixture, the reverse dependence suggests that the dehydrogenation rate depends on $[\text{HCOO}^-]$. In line with this, no gas bubble was observed in neat FA, and no Rh–H species was detected in neat FA, either (Figure S6). These observations appear to indicate that the dehydrogenation is rate-limited by the step of hydride formation, where coordination of the formate is necessary.

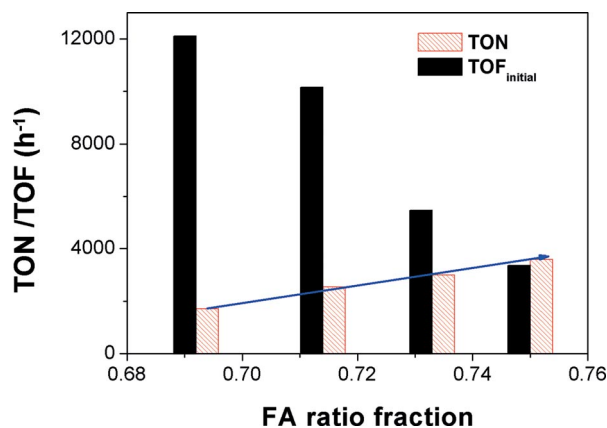


Figure 3. TON and TOF values observed in FT solutions with various FA/TEA ratios. Conditions: 0.8 μmol of $[\text{RhCp}^*\text{Cl}_2]_2$, 320 μmol of KI, 1.5 mL of FT mixture solution with varying FA/TEA ratio in the range 2.25:1 to 3:1, 60 °C. Each data is the average value of two runs, and the TON was measured by using the final gas amount as shown in Figure S5, from 20 to 50 min. The TOF was calculated on the basis of the volume of evolved gas from 3 to 6 min after the beginning of the reaction, to rule out the influence of temperature fluctuation due to the injection of FT solution and to avoid the initial induction period.

In addition to TEA, other amines were also tested for the reaction (Figure S7). Tertiary amines show superior reactivity compared with primary and secondary amines. This may be because the latter two types of amines are better hydrogen-bond donors, reducing the concentration of free iodide ions needed for higher dehydrogenation rates (vide supra).

The Structure of Active Catalysts

Next, efforts were made to investigate the role of I^- in this reaction. Firstly, a contrast experiment was conducted by using $[\text{RhCp}^*\text{Cl}_2]_2$ and $[\text{RhCp}^*\text{I}_2]_2$ as catalyst precursors. As shown in Figure 4, without KI, the FA dehydrogenation rates for both rhodium complexes are low and essentially identical. When KI is added, both reactions are accelerated considerably and to a similar extent. These findings rule out the possibility that the iodide effect arises from the iodide-ligated rhodium dimer, $[\text{RhCp}^*\text{I}_2]_2$, and suggest that the same active catalyst is generated in the presence of I^- regardless of which rhodium precursor is used. The necessity for a large excess of coordinating I^- also indicates that the active catalyst is less likely to be other forms of dimeric $\text{Cp}^*\text{Rh}^{\text{III}}-\text{I}$ species. It is noted that replacing KI

with the same amount of KCl has only an insignificant effect on the dehydrogenation catalyzed by $[\text{Cp}^*\text{RhI}_2]_2$ (Figure S8).

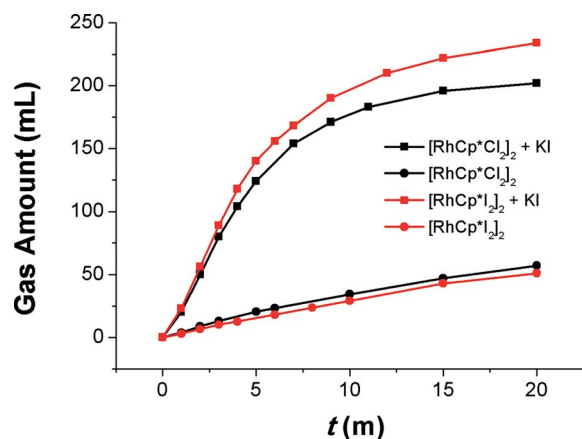


Figure 4. FA dehydrogenation with $[\text{RhCp}^*\text{Cl}_2]_2$ and $[\text{RhCp}^*\text{I}_2]_2$ (5.0 μmol of $[\text{RhCp}^*\text{X}_2]_2$, 1 mmol of KI when added, 1.5 mL of FT azeotrope, 60 °C).^[7]

We also monitored the FA dehydrogenation with $[\text{RhCp}^*\text{Cl}_2]_2$ at room temperature in the absence or presence of I^- by ^1H NMR spectroscopy over a period of 72 h (Figure S9; for details see the Experimental Section). Comparing Figures S9a and S9b shows that the FA (indicated by the formate proton signal) was consumed to a greater extent after 72 h in the presence of I^- (54 % vs. 18 % FA conversion), which is consistent with the results from Figure 1. Figure 5 shows the hydride part ($\delta = -5$ to

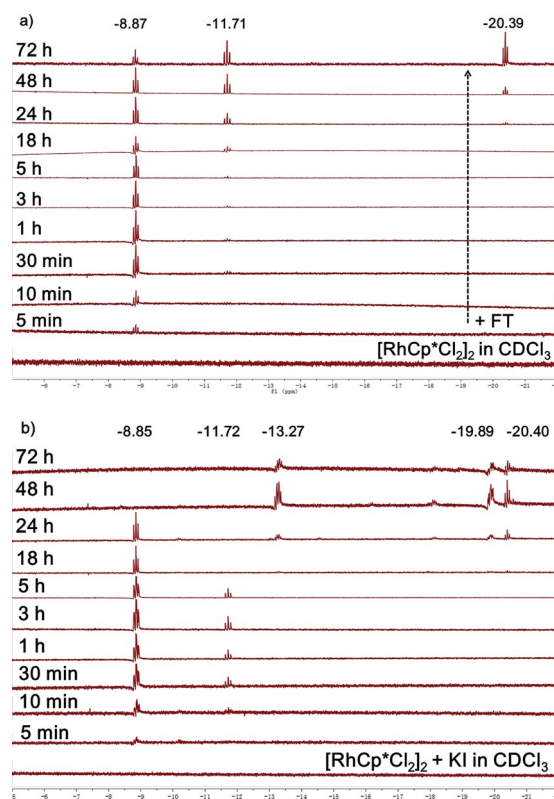


Figure 5. ^1H NMR spectra of the reaction mixture of $[\text{RhCp}^*\text{Cl}_2]_2$ with FT azeotrope in CDCl_3 (hydride part): (a) without KI; (b) in the presence of KI (250 μmol). General conditions: 5.0 μmol of $[\text{RhCp}^*\text{Cl}_2]_2$, 0.1 mL of FT azeotrope, room temperature. Timing started after the injection of FT solution.

–22 ppm) of Figure S9 (enlarged). Without KI (Figure 5a), a Rh–H hydride triplet at $\delta = -8.87$ ppm along with a new chemical shift at $\delta = 1.90$ ppm [Cp* proton, Figure S9e] appeared instantly (less than 5 min) upon mixing the rhodium precursor with the FT azeotrope in CDCl₃, indicating quick formation of a binuclear rhodium species with a bridging hydride.^[8] Other rhodium species bearing bridging hydride ligands started to appear later ($\delta = -11.71$ and -20.39 ppm). In the presence of KI (Figure 5b), the NMR spectra show that similar rhodium species are formed quickly in addition to a new peak at $\delta = -8.85$ ppm, which overlaps with a slightly smaller peak centered at $\delta = -8.87$ ppm [Figure S9g]. The latter peak presumably arises from the same species as that in the absence of the iodide. However, the peak at $\delta = -11.72$ ppm disappeared after 5 h while that at $\delta = -8.85$ ppm disappeared after 24 h, accompanied with the appearance of new, unknown rhodium species with bridging hydride. It is also worth noting that there is no visible doublet hydride resonance during the catalytic reaction, again indicating that the dehydrogenation is likely to be turnover-limited by the step of hydride formation. Since gas evolution was observed over the entire period of 72 h in both cases, the disappearance of the triplets mentioned is consistent with the corresponding binuclear rhodium species not being the active catalyst.

Mass spectrometry was then employed in an attempt to identify these rhodium species. Figure 6 shows the mass fragment of [RhCp*Cl₂]₂ reacting with the FT azeotrope in methanol within 5 min of the beginning of the reaction (also see Figure S10). In the absence of KI, the mass peak at $m/z = 557.0228$

can be ascribed to [Rh₂Cp*₂Cl(H)(OCHO)]⁺ (**d**, Scheme 1, vide infra), a rhodium dimer complex containing a bridging hydride and a bridging formate ligand (¹H NMR: $\delta = 7.39$ ppm).^[9] When KI was added, the newly generated mass peak at $m/z = 648.9554$ supports the formation of [Rh₂Cp*₂I(H)(OCHO)]⁺ (**D**, Scheme 1),^[10] an analogue of **d**, while that at $m/z = 730.8639$ may correspond to [Rh₂Cp*₂(H)I₂]⁺ (**E**, Scheme 1).^[11] Each of these species is expected to display a triplet hydride signal in

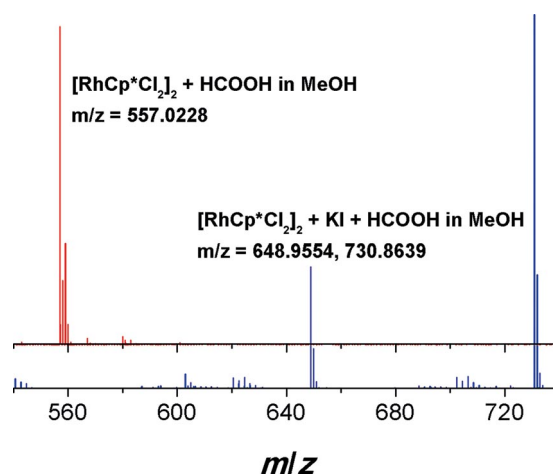
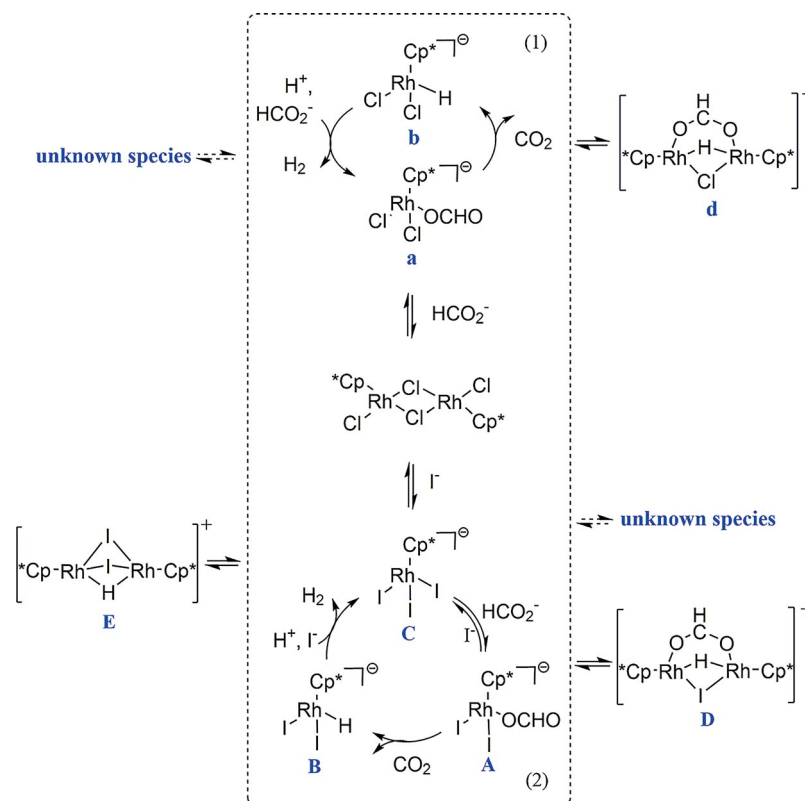


Figure 6. Mass spectrum of the reaction mixture of [RhCp*Cl₂]₂ with FT azeotrope in methanol (1.6 μ mol of [RhCp*Cl₂]₂, 0.2 mL of FT azeotrope, 1.0 mL of methanol, room temperature). Top: without KI; bottom: with 120 μ mol of KI.



Scheme 1. Plausible reaction mechanism for the dehydrogenation of FA with [RhCp*Cl₂]₂ in the absence (1) or presence (2) of I⁻.

its ^1H NMR spectrum and thus appears to correspond well to those revealed in Figure 5.

Proposed Mechanism

Taken together, a plausible reaction mechanism is tentatively suggested for the dehydrogenation of FA catalyzed by $[\text{RhCp}^*\text{Cl}_2]_2$ (Scheme 1). With or without KI, the dimeric $[\text{RhCp}^*\text{Cl}_2]_2$ firstly dissociates under the reaction conditions, turning into the catalytically active monomeric rhodium species **a** in the absence of I^- and **C** in its presence.^[12] The latter is in fast equilibrium with formate **A**, the iodo analogue of **a**. Subsequently, rhodium hydrides **b** and **B** are formed from **a** and **A** by decarboxylation; their protonation releases H_2 and regenerates the active catalysts. During the catalytic turnover, the spectator dimeric species **d**, **D**, and **E**, containing bridging hydride, are formed upon dimerization of the monomers in the catalytic cycle. As the reaction progresses, other unknown rhodium species are formed, as shown in the ^1H NMR spectra in Figure 5.^[13] These species are not considered as reactive species. However, they may be in fast equilibrium with the catalytically active monomers; otherwise, the catalyst would deactivate quickly.^[9a] As indicated above, the overall dehydrogenation is likely to be controlled by the step of hydride formation in turnover.^[14,15] Thus, the promoting effect of iodide can be ascribed to the fact that decarboxylation from **A** is easier than that from **a**, which in turn may be because iodide is a better ligand to Rh^{III} than chloride.^[17] Since the decarboxylation could proceed via a transition state involving dissociation of the formate to form an ion pair,^[4a,15,16] a better coordinating iodide anion would be expected to stabilize the transition state that contains a positively charged Rh^{III} better. However, an excess amount of iodide will shift the equilibrium between **C** and **A** to favor **C**, thereby giving rise to the saturation kinetics observed (Figure 2).

Stability of the Catalyst

The stability of this catalyst system for FA dehydrogenation was also investigated. During a single FA decomposition reaction with $5.0\ \mu\text{mol}$ of $[\text{RhCp}^*\text{Cl}_2]_2$ and $1.0\ \text{mmol}$ of KI in $1.5\ \text{mL}$ of FT azeotrope at $60\ ^\circ\text{C}$, the catalyst is observed to lose activity eventually (at conversion values less than 50 %, Figure 1), and gas evolution could not be fully recovered with the addition of either FA or FT azeotrope (Figure S11). This could be caused by the irreversible formation of some deactivated rhodium hydride species as a result of the consumption of FA (Figure S12). Nevertheless, the addition of KI prolongs the lifetime (TON) of the catalytic system; in its absence, the catalyst has low activity right from the beginning (Figure 4). One way to keep this reaction going is to add an additional amount of FA into the system at certain time intervals. This is shown in Figure 7, where more than 1000 mL of H_2 were released upon seven consecutive additions of FA, although the dehydrogenation rate became progressively slower. Thus, the TON was enhanced from 706 (Table 1) to over 2540.

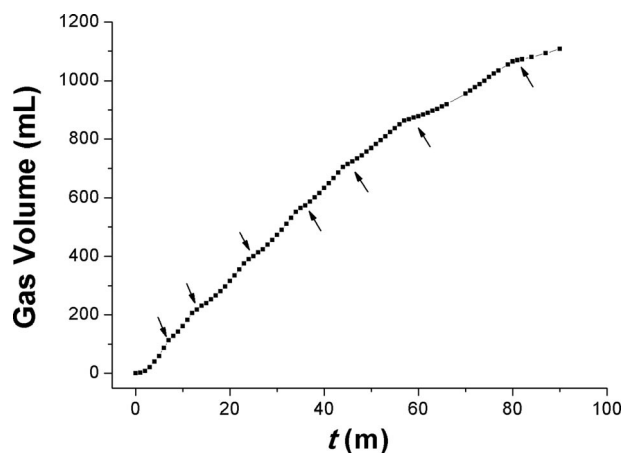


Figure 7. Longer-time reaction with intermittent addition of FA ($5.0\ \mu\text{mol}$ of $[\text{RhCp}^*\text{Cl}_2]_2$, $1.0\ \text{mmol}$ of KI, $1.5\ \text{mL}$ of FT azeotrope, $60\ ^\circ\text{C}$). The amount of FA added was roughly based on the amount of evolved gas (0.12, 0.12, 0.12, 0.12, 0.12, 0.15, and 0.15 mL).

Conclusions

The dehydrogenation of FA catalyzed by a simple, readily available rhodium catalyst is reported. The activity of the $[\text{RhCp}^*\text{Cl}_2]_2$ catalyst is enhanced by the addition of halide ions. The catalytic activity increases with the atomic number of halide ions, and with I^- , the activity is increased to sevenfold that without added halide. Not only does the iodide ion increase the reaction rate, but it also prolongs the catalyst lifetime. Kinetic studies and NMR spectroscopic monitoring suggest that the active catalyst is mononuclear and is in equilibrium with binuclear hydrides outside of the catalytic cycle. The catalytic turnover appears to be controlled by the rate of hydride formation, which is facilitated by iodide anions coordinated to the Rh^{III} center.

Experimental Section

General: The ^1H NMR spectra were recorded with a Bruker Avance 400 NMR spectrometer. GC analysis results were obtained from Techcomp GC7890II (equipped with a TCD or FID detector and methanizer). HRMS data were recorded with a Finnigan MAT 95 system. The FT azeotrope was distilled prior to use. $[\text{RhCp}^*\text{I}_2]_2$ was prepared according to the literature.^[18]

Procedure of FA Dehydrogenation: $[\text{RhCp}^*\text{Cl}_2]_2$ and KI were placed in a thick-walled reaction vessel fitted with a side tube and a rubber septum. The vessel was then preheated to a given temperature by means of an oil bath under ambient atmosphere. FT azeotrope ($1.5\ \text{mL}$) was injected through the septum; 5 seconds later, stirring and timing were started. The side arm of the vessel was connected to a gas collection apparatus (standard water displacement apparatus, with a graduated cylinder to determine volume), and the volume of the evolved gas was recorded. The products of FA decomposition were confirmed to be H_2 and CO_2 in a ratio of 1:1 with no observable evolution of CO .

Calculation of TONs and TOFs

The TON was calculated by Equation (1). The total gas volume was corrected by taking into account the expansion of gas due to the injection of FT azeotrope ($1.5\ \text{mL}$) into the preheated vessel and

also the contributions from the solvent and water vapor (an average value of 1.5 mL gas), which were measured in an experiment without the catalyst. At room temperature, $V_{m,20\text{ }^\circ\text{C}} = 24\text{ L mol}^{-1}$ (see the Supporting Information).

$$\text{TON} = [V_{\text{total}} / (2 \times V_{m,20\text{ }^\circ\text{C}})] / n_{\text{cat}} (1)$$

where n denotes number of mol, and $n_{\text{cat}} = 2 n_{\text{dimer}}$

The calculation of TOF is time-related (h^{-1}) and based on the TON value. For example: using 0.8 μmol of $[\text{RhCp}^*\text{Cl}_2]_2$ and 320 μmol of KI in 1.5 mL of FT (2.25:1) solution, 42 mL of gas was released at 60 $^\circ\text{C}$ in 2 min, thus:

$$\text{TOF} = [42 / (2 \times 24) \times 1000] / (1.6) \times 30 = 16406\text{ h}^{-1}.$$

NMR Spectroscopic Study of FA Dehydrogenation: At room temperature, FA dehydrogenation catalyzed by $[\text{RhCp}^*\text{Cl}_2]_2$ with or without I^- was tracked up to 72 h by ^1H NMR spectroscopy (Figure S8). For reaction without KI, $[\text{RhCp}^*\text{Cl}_2]_2$ (5.0 μmol) was dissolved in CDCl_3 (1.0 mL) first. Then, FT azeotrope (0.1 mL) was introduced, and gas bubbles were observed upon shaking immediately. The NMR tube was sealed and inserted into the spectrometer immediately to obtain the first ^1H NMR spectrum. The NMR spectra at other times (from 5 min to 72 h) were collected subsequently. For reaction with KI, $[\text{RhCp}^*\text{Cl}_2]_2$ (5.0 μmol) and KI (250 μmol) were mixed in CDCl_3 (1.0 mL) first. When FT azeotrope (0.1 mL) was added, gas bubbles were observed upon shaking immediately. The same procedure as that described above was followed.

Recording Mass Spectra for FA Dehydrogenation: The catalyst ($[\text{RhCp}^*\text{Cl}_2]_2$ or $[\text{RhCp}^*\text{Cl}_2]_2 + \text{KI}$) was dissolved in methanol first. Then, the FT azeotrope was injected into the vial. After shaking the vial, the MS analysis was performed. All of the spectra were recorded within 5 min after addition of the FT azeotrope (Figure S9).

Acknowledgments

We thank the Dalian Institute of Chemical Physics (DICP) – University of Liverpool – British Petroleum (BP) joint PhD program for a studentship and British Petroleum (BP) for financial support (Z. W.).

Keywords: Dehydrogenation · Rhodium · Homogeneous catalysis · Formic acid · Halides

- [1] For reviews, see: a) P. Makowski, A. Thomas, P. Kuhn, F. Goettmann, *Energy Environ. Sci.* **2009**, *2*, 480–490; b) H. L. Jiang, S. K. Singh, J. M. Yan, X. B. Zhang, Q. Xu, *ChemSusChem* **2010**, *3*, 541–549; c) A. F. Dalebrook, W. Gan, M. Grasemann, S. Moret, G. Laurenczy, *Chem. Commun.* **2013**, *49*, 8735–8751; d) M. Yadav, Q. Xu, *Energy Environ. Sci.* **2012**, *5*, 9698–9725; e) Q.-L. Zhu, Q. Xu, *Energy Environ. Sci.* **2015**, *8*, 478–512; f) F. Joo, *ChemSusChem* **2008**, *1*, 805–808.
- [2] For reviews, see: a) T. C. Johnson, D. J. Morris, M. Wills, *Chem. Soc. Rev.* **2010**, *39*, 81–88; b) M. Grasemann, G. Laurenczy, *Energy Environ. Sci.* **2012**, *5*, 8171–8181; c) E. Fujita, J. T. Muckerman, Y. Himeda, *Biochim. Biophys. Acta* **2013**, *1827*, 1031–1038; d) S. Enthaler, J. von Langermann, T. Schmidt, *Energy Environ. Sci.* **2010**, *3*, 1207–1217; e) S. Enthaler, *ChemSusChem* **2008**, *1*, 801–804; f) M. Czaun, A. Goepfert, R. May, R. Haiges, G. K. Prakash, G. A. Olah, *ChemSusChem* **2011**, *4*, 1241–1248; g) B. Loges, A. Boddien, F. Gärtner, H. Junge, M. Beller, *Top. Catal.* **2010**, *53*, 902–914.
- [3] For selected examples of heterogeneous FA dehydrogenation, see: a) Y. Huang, X. Zhou, M. Yin, C. Liu, W. Xing, *Chem. Mater.* **2010**, *22*, 5122–5128; b) X. Gu, Z.-H. Lu, H.-L. Jiang, T. Akita, Q. Xu, *J. Am. Chem. Soc.* **2011**, *133*, 11822–11825; c) K. Tedsree, T. Li, S. Jones, C. W. A. Chan, K. M. K. Yu, P. A. Bagot, E. A. Marquis, G. D. Smith, S. C. E. Tsang, *Nanotechnol.* **2011**, *6*, 302–307; d) S. Jones, J. Qu, K. Tedsree, X. Q. Gong, S. C. E. Tsang, *Angew. Chem. Int. Ed.* **2012**, *51*, 11275–11278; *Angew. Chem.* **2012**, *124*, 11437; e) Q.-Y. Bi, X.-L. Du, Y.-M. Liu, Y. Cao, H.-Y. He, K.-N. Fan, *J. Am. Chem. Soc.* **2012**, *134*, 8926–8933; f) Z.-L. Wang, J.-M. Yan, Y. Ping, H.-L. Wang, W.-T. Zheng, Q. Jiang, *Angew. Chem. Int. Ed.* **2013**, *52*, 4406–4409; *Angew. Chem.* **2013**, *125*, 4502; g) S. Zhang, O. Metin, D. Su, S. Sun, *Angew. Chem. Int. Ed.* **2013**, *52*, 3681–3684; *Angew. Chem.* **2013**, *125*, 3769; h) M. Yadav, T. Akita, N. Tsumori, Q. Xu, *J. Mater. Chem.* **2012**, *22*, 12582–12586; i) Q.-L. Zhu, N. Tsumoriab, Q. Xu, *Chem. Sci.* **2014**, *5*, 195–199; j) C. Feng, Y. Hao, L. Zhang, N. Shang, S. Gao, Z. Wang, C. Wang, *RSC Adv.* **2015**, *5*, 39878–39883; k) Y.-L. Qin, Y.-C. Liu, F. Liang, L.-M. Wang, *ChemSusChem* **2015**, *8*, 260–263; l) K. Koh, J.-E. Seo, J. H. Lee, A. Goswami, C. W. Yoon, T. Asefa, *J. Mater. Chem. A* **2014**, *2*, 20444–20449.
- [4] For selected examples of homogeneous FA dehydrogenation, see: a) C. Fellay, P. J. Dyson, G. Laurenczy, *Angew. Chem. Int. Ed.* **2008**, *47*, 3966–3968; *Angew. Chem.* **2008**, *120*, 4030; b) B. Loges, A. Boddien, H. Junge, M. Beller, *Angew. Chem. Int. Ed.* **2008**, *47*, 3962–3965; *Angew. Chem.* **2008**, *120*, 4026; c) A. Boddien, F. Gärtner, C. Federsel, P. Sponholz, D. Mellmann, R. Jackstell, H. Junge, M. Beller, *Angew. Chem. Int. Ed.* **2011**, *50*, 6411–6414; *Angew. Chem.* **2011**, *123*, 6535; d) M. Czaun, A. Goepfert, J. Ko-thandaraman, R. B. May, R. Haiges, G. K. S. Prakash, G. A. Olah, *ACS Catal.* **2014**, *4*, 311–320; e) G. A. Filonenko, R. V. Putten, E. N. Schulpen, M. E. J. Hensen, E. A. Pidko, *ChemCatChem* **2014**, *6*, 1526–1530; f) R. Tanaka, M. Yamashita, L. W. Chung, K. Morokuma, K. Nozaki, *Organometallics* **2011**, *30*, 6742–6750; g) Y. Manaka, W. H. Wang, Y. Suna, H. Kambayashi, J. T. Muckerman, E. Fujita, Y. Himeda, *Catal. Sci. Technol.* **2014**, *4*, 34–37; h) S. Fukuzumi, T. Kobayashi, T. Suenobu, *J. Am. Chem. Soc.* **2010**, *132*, 1496–1497; i) Z. Wang, S.-M. Lu, J. Li, J. Wang, C. Li, *Chem. Eur. J.* **2015**, *21*, 12592; j) J. F. Hull, Y. Himeda, W. H. Wang, B. Hashiguchi, R. Periana, D. J. Szalda, J. T. Muckerman, E. Fujita, *Nat. Chem.* **2012**, *4*, 383–388; k) J. H. Barnard, C. Wang, N. G. Berry, J. Xiao, *Chem. Sci.* **2013**, *4*, 1234–1244; l) A. Boddien, B. Loges, F. Gärtner, C. Torborg, K. Fumino, H. Junge, R. Ludwig, M. Beller, *J. Am. Chem. Soc.* **2010**, *132*, 8924–8934; m) A. Boddien, D. Mellmann, F. Gärtner, R. Jackstell, H. Junge, P. J. Dyson, G. Laurenczy, R. Ludwig, M. Beller, *Science* **2011**, *333*, 1733–1736; n) T. Zell, B. Butschke, Y. Ben-David, D. Milstein, *Chem. Eur. J.* **2013**, *19*, 8068–8072; o) E. A. Bielinski, P. O. Lagaditis, Y. Zhang, B. Q. Mercado, C. Wurtele, W. H. Bernskoetter, N. Hazari, S. Schneider, *J. Am. Chem. Soc.* **2014**, *136*, 10234–10237; p) F. Bertini, I. Mellone, A. Ienco, M. Peruzzini, L. Gonsalvi, *ACS Catal.* **2015**, *5*, 1254–1265; q) T. W. Myers, L. A. Berben, *Chem. Sci.* **2014**, *5*, 2771–2777; r) S. Enthaler, A. Brück, A. Kammer, H. Junge, E. Irran, S. Güllak, *ChemCatChem* **2015**, *7*, 65–69; s) S. Oldenhof, B. de Bruin, M. Lutz, M. A. Siegler, F. W. Patureau, J. I. van der Vlugt, J. N. H. Reek, *Chem. Eur. J.* **2013**, *19*, 11507.
- [5] a) K. Fagnou, M. Lautens, *Angew. Chem. Int. Ed.* **2002**, *41*, 26–47; *Angew. Chem.* **2002**, *114*, 26; b) P. M. Maitlis, A. Haynes, B. R. James, M. Catellani, G. P. Chiussoli, *Dalton Trans.* **2004**, *21*, 3409–3419.
- [6] a) J. Wu, C. Wang, W. Tang, A. Pettman, J. Xiao, *Chem. Eur. J.* **2012**, *18*, 9525–9529; b) J. Wu, W. Tang, A. Pettman, J. Xiao, *Adv. Synth. Catal.* **2013**, *355*, 35–40; c) Y. Wei, J. Wu, D. Xue, C. Wang, Z. Liu, Z. Zhang, G. Chen, J. Xiao, *Synlett* **2014**, *25*, 1295–1298; d) H. Junge, A. Boddien, F. Capitta, B. Loges, J. R. Noyes, S. Gladiali, M. Beller, *Tetrahedron Lett.* **2009**, *50*, 1603.
- [7] The catalytic activity here is slightly lower compared with that in Figure 1. A different bottle of $[\text{RhCp}^*\text{Cl}_2]_2$ was used.
- [8] C. Fischer, C. Kohrt, H.-J. Drexler, W. Baumann, D. Heller, *Dalton Trans.* **2011**, *40*, 4162–4166.
- [9] a) A. J. Blacker, S. B. Duckett, J. Grace, R. N. Perutz, A. C. Whitwood, *Organometallics* **2009**, *28*, 1435–1446; b) species **d** is one of the most possible configurations for $[\text{Rh}_2\text{Cp}^*_2\text{Cl}(\text{H})(\text{OCHO})]^+$; please see the Supporting Information.
- [10] Species **D** is one of the most possible configurations based on $[\text{Rh}_2\text{Cp}^*_2\text{IH}(\text{OCHO})]^+$; please see the Supporting Information.
- [11] Species **E** is one of the most possible configurations for $[\text{Rh}_2\text{Cp}^*_2\text{HI}_2]^+$; please see the Supporting Information.
- [12] Species **C** is one of the most possible speculated configurations, but without direct support from experimental data.
- [13] Those unknown multinuclear species could be the reservoir of the reactive species.
- [14] The possibility that the protonation step could be the RDS cannot be ruled out, however, as the equilibrium between the monomer and dimer

- could render the concentration of the monomeric Rh–H too low to be detected by ^1H NMR spectroscopy.
- [15] In line with this view, we have recently shown that hydride formation is more energy-costly than hydride transfer in a kinetic, NMR spectroscopic, and DFT study of an iridium-catalyzed transfer hydrogenation of imines with formic acid: H.-Y. T. Chen, C. Wang, X. Wu, X. Jiang, C. R. A. Catlow, J. Xiao, *Chem. Eur. J.* **2015**, *21*, 16564–16577.
- [16] For references on the ion pair mechanism, see: a) J. H. Merrifield, J. A. Gladysz, *Organometallics* **1983**, *2*, 782–784; b) S. Oldenhof, M. Lutz, B. de Bruin, J. I. van der Vlugt, J. N. H. Reek, *Chem. Sci.* **2015**, *6*, 1027–1034;
- c) A. Nova, D. J. Taylor, A. J. Blacker, S. B. Duckett, R. N. Perutz, O. Eisenstein, *Organometallics* **2014**, *33*, 3433–3442.
- [17] Although KBr and KCl also promote this reaction, their effect is much less significant than that of KI (Figure 1), probably because the iodide is softer and a stronger nucleophile in protic solvents and hence is expected to bind to the iridium more easily (see ref.^[5]).
- [18] W. D. Jones, F. J. Feher, *Inorg. Chem.* **1984**, *23*, 2376–2388.

Received: September 16, 2015
Published Online: January 12, 2016